

Two-gluon correlations and initial conditions for small- x evolution

Adrian Dumitru^{a,b,c}, Jamal Jalilian-Marian^{b,c}, Elena Petreska^{b,c}

^a *RIKEN BNL Research Center, Brookhaven National Laboratory, Upton, NY 11973, USA*

^b *Department of Natural Sciences, Baruch College,*

CUNY, 17 Lexington Avenue, New York, NY 10010, USA

^c *The Graduate School and University Center, City University of New York, 365 Fifth Avenue, New York, NY 10016, USA*

We derive the effective action of the hard large- x valence charges up to fourth order in their density. Such non-Gaussian weight functionals contribute at leading order in N_c to the connected two-gluon production diagrams which determine di-hadron correlations. The corresponding diagrams are not necessarily (highly) suppressed by the density of valence charges since their infrared divergences differ from those obtained in a Gaussian theory. Therefore, it appears prudent to include such higher dimensional operators when determining initial ensembles for JIMWLK evolution of higher n -point functions of Wilson lines.

I. INTRODUCTION

(Multi-) Particle production cross sections in hadronic collisions at high energies are related to expectation values of traces of products of Wilson lines which resum multiple scattering and high gluon density effects. The evolution of such operator expectation values is described by the JIMWLK functional renormalization group equation [1]. In the large- N_c limit, and in a Gaussian approximation for the effective action, they reduce to the BK equation [2] for the dipole forward scattering amplitude.

The high-energy evolution equations require initial conditions at a rapidity $Y = \log x_0/x = 0$ (x_0 is often assumed to be about 10^{-2}). They have been derived by McLerran and Venugopalan [3] in the limit of an infinitely large nucleus. In the MV model, the large- x valence charges act as recoilless sources for the soft, small- x gluon fields. As $A \rightarrow \infty$ then, the variance of the “valence” charge density $\sim A^{1/3}$ grows large and the distribution of color charges should be Gaussian,

$$S_{\text{MV}} = \int d^2x_{\perp} \frac{\text{tr} \rho^2(x_{\perp})}{\mu^2} = \int d^2x_{\perp} \frac{\delta^{ab} \rho^a(x_{\perp}) \rho^b(x_{\perp})}{2\mu^2} \quad , \quad \mu^2 \sim \frac{g^2 A}{\pi R^2} . \quad (1)$$

It should be noted that high multiplicity proton-proton collisions may also correspond to unusually high valence charge densities (see, for example, ref. [4]) and so would also be described effectively by this action with $A_{\text{eff}} \gg 1$.

Nevertheless, in reality the mass number A resp. the number of valence charges is finite, in particular in (high-multiplicity) pp as well as peripheral AA collisions. It is therefore interesting to consider extensions of the MV-model action involving higher powers of the color charge density. In fact, Jeon and Venugopalan have derived [5] an “odderon” operator contribution $-d^{abc} \rho^a \rho^b \rho^c / \kappa_3$, where the cubic coupling $\kappa_3 \sim g^3 (A/\pi R^2)^2$. Below, we shall show that at quartic order in ρ a contribution $\delta^{ab} \delta^{cd} \rho^a \rho^b \rho^c \rho^d / \kappa_4$ to the effective action arises, with $\kappa_4 \sim g^4 (A/\pi R^2)^3$.

Our motivation derives from the recent observation of a “ridge” in two-particle correlations from high-multiplicity pp [6] as well as heavy-ion collisions [7]. The ridge refers to a correlation which extends over several units¹ of (relative) rapidity for particles with similar azimuthal angle, $\Delta\phi \ll \pi$. For high-multiplicity pp collisions at $\sqrt{s} = 7$ TeV the CMS collaboration found that the amplitude of the “ridge” correlation peaks about transverse momenta on the order of 2-3 GeV, a semi-hard scale. Ref. [8] argued that within the framework of high energy evolution this effect would correspond to production of two small- x gluons with relative rapidity $\Delta y \gtrsim 1$ from two evolution ladders which connect to the same large- x sources [10, 11].

With a Gaussian action one finds that the two-particle distribution minus the product of two single-particle distributions,

$$\frac{\left\langle \frac{dN_p}{d^2p dy_p} \frac{dN_q}{d^2q dy_q} \right\rangle}{\left\langle \frac{dN}{d^2p dy_p} \right\rangle \left\langle \frac{dN}{d^2q dy_q} \right\rangle} - 1 \sim \frac{1}{N_c^2 - 1} \quad (2)$$

¹ It is presently not known whether the correlation simply satisfies boost invariance or whether it diminishes for rapidity intervals on the order of $1/\alpha_s$ [8, 9].

is suppressed by a factor $1/(N_c^2 - 1)$ relative to the uncorrelated part $\left\langle \frac{dN}{d^2p dy_p} \right\rangle \left\langle \frac{dN}{d^2q dy_q} \right\rangle$. At this subleading order in N_c , however, Gaussian factorization of the four-point function which determines (2) is violated by JIMWLK evolution [12].

This problem could be cured by a dynamically generated correlation length (in the transverse plane) of small- x gluon fields [13]. For a discussion of how color charge correlations develop as a hadron or nucleus is boosted to high rapidity we refer to ref. [14]. Averaging of n -point functions of Wilson lines with a local Gaussian would not apply when those n points are within one correlation length of each other and consequently a connected contribution should arise at leading order in N_c [13]. This can be seen also from a model which assumes splitting of the four-point function into two-point functions (“ladders”) with non-zero individual transverse momenta [15].

Here, we show that a non-Gaussian initial distribution of valence charge naturally arises when $A < \infty$ and that it leads to particle correlations at leading order in N_c . Furthermore, that the infrared behavior of the leading connected two-particle production diagram is different from the case of a quadratic action. This fact may affect the relative A -dependence of the correlations resulting from the quadratic vs. the higher-order terms in the action.

We focus on the kinematic regime where the transverse momenta p, q of the two produced gluons are somewhat larger than *but on the order of* the scale where evolution in rapidity is non-linear. For a proton, this so-called saturation scale $Q_s(x)$ is expected to be on the order of 1 GeV at $x \approx$ a few times 10^{-4} , on average; high-multiplicity collisions should correspond to configurations with significantly higher parton densities. For nuclei, the valence charge density should be boosted by a factor of $\sim A^{1/3}$. In this kinematic regime, the transverse momenta of the produced gluons are, to a significant part, due to the intrinsic transverse momentum from the small- x evolution ladders. Further, the relative azimuthal angle of \mathbf{p} and \mathbf{q} is taken to be small, $\Delta\phi \ll \pi$.

When $\log p^2/Q_s^2 \gg 1$ and $\log q^2/Q_s^2 \gg 1$ the situation is different. This case has been analyzed within the double-logarithmic approximation in ref. [16]. They show that here a single “flip” (or “recombination”) between the two evolution ladders is suppressed and that *two* such flips are required, one below and the other above the rapidities of the produced $d\bar{i}$ -jets. At very high energies such flips between ladders may occur at a hard transverse momentum scale not too far from the hard dijet vertices themselves [16].

II. DERIVATION OF THE EFFECTIVE ACTION BEYOND QUADRATIC ORDER

In this section we derive the form of the effective action for a system of k quarks in SU(3) following the methods developed in [5]. The probability to find this system in a representation labeled by the integers (m, n) , also denoted as Dynkin labels, is given by $d_{mn} N_{m,n}^{(k)}$ where

$$e^{-S} \equiv d_{m,n} N_{m,n}^{(k)} = d_{m,n} \left[G_{m,n}^{(k)} + G_{m+3,n}^{(k)} + G_{m,n+3}^{(k)} - G_{m+2,n-1}^{(k)} - G_{m-1,n+2}^{(k)} - G_{m+2,n+2}^{(k)} \right] \quad (3)$$

with

$$G_{k:m,n} = \frac{k!}{\left(\frac{k+2m+n}{3}\right)! \left(\frac{k-m+n}{3}\right)! \left(\frac{k-m-2n}{3}\right)!} . \quad (4)$$

We are interested in the representation with the largest weight and so consider the limit $k \gg m, n \gg 1$. Thus, we expand the factorials in each G in powers of $1/k$ up to and including order $\sim \frac{1}{k^3}$. The leading terms of the form $\sim \frac{m^j n^{l+1-j}}{k^l}$ can be written as

$$S(m, n; k) \simeq \frac{N_c}{k} C_2(m, n) - \frac{1}{3} \left(\frac{N_c}{k}\right)^2 C_3(m, n) + \frac{1}{6} \left(\frac{N_c}{k}\right)^3 C_4(m, n) \quad (5)$$

where C_2, C_3, C_4 are the SU(3) Casimir operators for the representation (m, n) , given by (see appendix)

$$C_2(m, n) \equiv \frac{1}{3} (m^2 + n^2 + mn) + (m + n) \quad (6)$$

$$C_3(m, n) \equiv \frac{1}{18} (m + 2n + 3) (n + 2m + 3) (m - n) \quad (7)$$

$$C_4(m, n) \equiv \frac{1}{9} (m^4 + n^4 + 2mn^3 + 2m^3n + 3m^2n^2) + \frac{2}{3} (m^3 + n^3 + 2m^2n + 2mn^2) + \frac{1}{6} (5m^2 + 5n^2 + 11mn) - \frac{1}{2} (m + n) . \quad (8)$$

Before we rewrite the action $S(m, n; k)$ in terms of the color charges ρ , it is perhaps useful to remind the reader of this derivation and to illustrate it in the simpler case of SU(2) spins [5]. In this case, the representation R is labeled by one index, l , and there is only one independent Casimir defined as $C_2(R)\mathbb{1}_R = \delta^{ab} L_R^a L_R^b = L_R^2$, where L_R^a are the generators of the representation R . For a large representation we have $C_2 = \ell(\ell + 1) \simeq \ell^2$ as the quadratic Casimir. One can then write $\ell^2 = \ell_i \ell_i$ where ℓ_i is a vector describing spin and express the action in terms of invariants formed by multiplying ℓ_i 's (in this example, there is only one invariant, ℓ^2) as $S \simeq N_c \ell^2 / k$. For large ℓ , one introduces a classical charge density per unit transverse area, $\rho^i(x) = g \ell^i / \Delta^2 x$. Next, k is expressed in terms of number of valence quarks in a nucleus as $k = N_c A \Delta^2 x / \pi R^2$ which then leads to

$$S = \frac{N_c}{k} \ell^2 \simeq \int d^2 x \frac{\rho^a \rho^a}{2\mu^2} \quad (9)$$

with $\mu^2 \equiv \frac{g^2 A}{2\pi R^2}$.

We start by defining the Casimirs for general N_c in terms of the generators $T_R^{a_i}$ of the representation R ,

$$C_n(R)\mathbb{1}_R \equiv F_R^{a_1, \dots, a_n} T_R^{a_1} \dots T_R^{a_n}, \quad (10)$$

where $\mathbb{1}_R$ is the unit matrix in the representation R . Taking the trace of both sides gives $C_n(R)$, the n^{th} Casimir of the representation R :

$$C_n(R) = \frac{1}{d_R} F_R^{a_1, \dots, a_n} \text{tr} T_R^{a_1} \dots T_R^{a_n}. \quad (11)$$

The color tensors $F_R^{a_1, \dots, a_n}$ are the most general color invariant tensors one can construct out of the SU(N_c) orthonormal basis tensors. For example, $F_R^{a_1, a_2} = \delta^{a_1, a_2}$ for $n = 2$, while for $n = 4$ these basis tensors are given by $\delta^{ab} \delta^{cd}$ plus permutations, $d^{abe} d^{cde}$ plus permutations, and $d^{abe} f^{cde}$ plus permutations. More explicitly,

$$\begin{aligned} C_2(R) &= \frac{1}{d_R} \delta^{ab} \text{tr} T_R^a T_R^b \\ C_3(R) &= \frac{1}{d_R} d^{abc} \text{tr} T_R^a T_R^b T_R^c \\ C_4(R) &= \frac{1}{d_R} [\alpha(\delta^{ab} \delta^{cd} + \delta^{ac} \delta^{bd} + \delta^{ad} \delta^{bc}) + \beta(d^{abe} d^{cde} + d^{ace} d^{bde} + d^{ade} d^{bce})] \text{tr} T_R^a T_R^b T_R^c T_R^d \end{aligned} \quad (12)$$

Since the number of independent Casimirs of SU(N_c) is equal to its rank, $N_c - 1$, there are only 2 independent Casimirs for SU(3). These are usually taken to be C_2 and C_3 . This can be seen explicitly by noting that for $N_c = 3$ one has the constraint

$$d^{abe} d^{cde} + d^{ace} d^{bde} + d^{ade} d^{bce} = \frac{1}{3} (\delta^{ab} \delta^{cd} + \delta^{ac} \delta^{bd} + \delta^{ad} \delta^{bc}) \quad (13)$$

and $3\alpha + \beta = 1$ so that the quartic Casimir can be written as the square of the quadratic invariant. To proceed, we write the action in terms of Q^a , a $N_c^2 - 1$ dimensional vector related to the second Casimir via $|Q| = \sqrt{Q^a Q^a} \equiv \sqrt{C_2}$; the vector Q^a is analogous to the angular momentum vector ℓ^a in our SU(2) example from above:

$$S \simeq \left[\frac{N_c}{k} Q^a Q^a - \left(\frac{N_c}{k} \right)^2 \frac{d^{abc}}{3} Q^a Q^b Q^c + \left(\frac{N_c}{k} \right)^3 \frac{\delta^{ab} \delta^{cd} + \delta^{ac} \delta^{bd} + \delta^{ad} \delta^{bc}}{18} Q^a Q^b Q^c Q^d \right]$$

We then follow McLerran-Venugopalan and define the color charge per unit area $\rho^a \equiv g Q^a / \Delta^2 x$ to finally arrive at

$$S[\rho(x)] \simeq \int d^2 x \left[\frac{\delta^{ab} \rho^a \rho^b}{2\mu^2} - \frac{d^{abc} \rho^a \rho^b \rho^c}{\kappa_3} + \frac{\delta^{ab} \delta^{cd} + \delta^{ac} \delta^{bd} + \delta^{ad} \delta^{bc}}{\kappa_4} \rho^a \rho^b \rho^c \rho^d \right]. \quad (14)$$

To write the action in this form we have used eq. (13) and $k = N_c A \frac{\Delta^2 x}{\pi R^2}$. This assumes that the large- x sources correspond to $N_c A$ valence quarks. On the other hand, if initial conditions for small- x evolution are set at, say, $x_0 = 0.01$ then the number of ‘‘valence’’ charges would be bigger although still parametrically proportional to A and to N_c .

The couplings in this action are given by, parametrically,

$$\mu^2 \equiv \frac{g^2 A}{2\pi R^2} \sim O(g^2 A^{1/3}), \quad (15)$$

$$\kappa_3 \equiv 3 \frac{g^3 A^2}{(\pi R^2)^2} \sim O(g^3 A^{2/3}), \quad (16)$$

$$\kappa_4 \equiv 18 \frac{g^4 A^3}{(\pi R^2)^3} \sim O(g^4 A). \quad (17)$$

The non-Gaussian terms in the action thus involve additional inverse powers of $gA^{1/3}$. Also, the expressions from above are obtained by averaging over the transverse (impact parameter) plane; at a fixed distance b from the center of a nucleus one should replace $A/\pi R^2$ by the thickness function $T(b)$.

The action (14) is coupled to the soft gauge fields [1]. At leading order and in the classical approximation this leads to the relation (22) below.

III. TWO-POINT FUNCTION AND UNINTEGRATED GLUON DISTRIBUTION

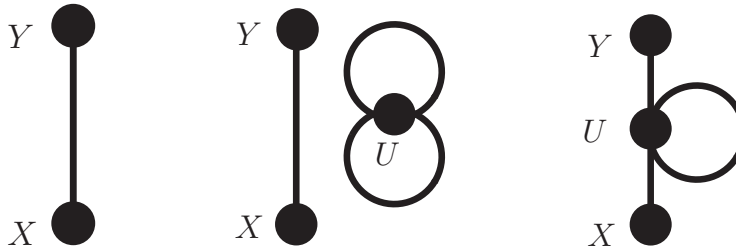


FIG. 1: Two-point function at leading order in $1/\kappa_4$.

In order to compute the contribution of the quartic term to a physical observable, such as single-inclusive hadron production in the forward region [17], one needs to perform the color averaging of the dipole operator with this new action: within the Glauber-Mueller approach the expectation value of the full dipole operator $\langle \text{tr } V_x V_y^\dagger \rangle$, where V denotes a Wilson line, resums multiple scattering effects on a dense target [2]. This can in principle be done numerically using lattice gauge theory methods [18]. Nevertheless, it is useful to consider a limit where this expectation value can be evaluated analytically, such as the dilute limit of the dipole cross section given by the two-point function of color charges. Even then, one can not perform the integration over ρ analytically when the action is not quadratic. We therefore resort to a perturbative expansion in $1/\kappa_4$ and keep only the first term in the expansion of the exponential of the quartic term. We then compute the two-point function of the color charge density of hard sources which is related to the unintegrated gluon distribution. To first non-trivial order in $1/\kappa_4$,

$$\langle O[\rho] \rangle \equiv \frac{\int \mathcal{D}\rho O[\rho] e^{-S_G[\rho]} \left[1 - \frac{1}{\kappa_4} \int d^2u \rho_u^a \rho_u^a \rho_u^b \rho_u^b \right]}{\int \mathcal{D}\rho e^{-S_G[\rho]} \left[1 - \frac{1}{\kappa_4} \int d^2u \rho_u^a \rho_u^a \rho_u^b \rho_u^b \right]}. \quad (18)$$

Here, S_G denotes the Gaussian action. For the two-point function $O = \rho_x^a \rho_y^b$, the possible contractions are shown diagrammatically in fig. 1; for the denominator of eq. (18) one amputates the points x and y . We compute the functional integral in lattice regularization, i.e. we approximate the two-dimensional transverse space by a lattice with N_s sites of area $\Delta^2 x$. The two-point function becomes²

$$\langle \rho_x^a \rho_y^b \rangle = \mu^2 \frac{\delta^{ab} \delta_{xy}}{\Delta^2 x} \frac{1 - \frac{\mu^4}{\kappa_4} (N_c^2 + 1)(N_c^2 - 1) \frac{N_s}{\Delta^2 x} - 4 \frac{\mu^4}{\kappa_4} (N_c^2 + 1) \frac{1}{\Delta^2 x}}{1 - \frac{\mu^4}{\kappa_4} (N_c^2 + 1)(N_c^2 - 1) \frac{N_s}{\Delta^2 x}}. \quad (19)$$

The disconnected contribution exhibits both a UV ($\Delta^2 x \rightarrow 0$) as well as a IR ($N_s \rightarrow \infty$) divergence but appears both in the numerator and in the denominator and so cancels as usual. The third term in the numerator is due to the tadpole diagram from fig. 1 which renormalizes the “bare” parameter μ^2 :

$$\tilde{\mu}^2 \equiv \mu^2 \left(1 - 4 \frac{\mu^4}{\kappa_4} \frac{N_c^2 + 1}{\Delta^2 x} \right). \quad (20)$$

This renormalization of μ^2 will be applied to all diagrams to absorb the insertion of a tadpole into any line.

² The right-hand-side of this expression is to be understood in lattice notation: x and y are discrete points and δ_{xy} is a Kronecker symbol.

Thus, the two-point function now reads (in continuum notation)

$$\langle \rho_x^a \rho_y^b \rangle = \tilde{\mu}^2 \delta^{ab} \delta(x-y) \leftrightarrow \langle \rho^{*a}(k) \rho^b(k') \rangle = \tilde{\mu}^2 \delta^{ab} (2\pi)^2 \delta(k-k'). \quad (21)$$

To relate (21) to the unintegrated gluon distribution we note that at leading order and in covariant gauge the field generated by a fast particle moving in the positive z -direction is related to the charge density by

$$A^\mu(x) \equiv \delta^{\mu+} \alpha(x) = g \delta^{\mu+} \delta(x^-) \frac{1}{\nabla_\perp^2} \rho(x), \quad (22)$$

where again x denotes a transverse coordinate. This field also satisfies $A^- = 0$ and so the only non-vanishing field-strength is $F^{+i} = -\partial^i \alpha$. In momentum space we have the relation $k^2 \alpha(k) = g \rho(k)$. Thus, we define the unintegrated gluon distribution $\Phi(k^2) \sim k^2 \langle F^{+i} F^{+i} \rangle$ via

$$\langle \rho^{*a}(k) \rho^b(k') \rangle = \frac{1}{\alpha_s} \frac{\delta^{ab}}{N_c^2 - 1} (2\pi)^3 \delta(k-k') \Phi(k^2). \quad (23)$$

With this convention, $\Phi(k^2) = \alpha_s (N_c^2 - 1) \tilde{\mu}^2 / (2\pi)$.

IV. FOUR-POINT FUNCTION

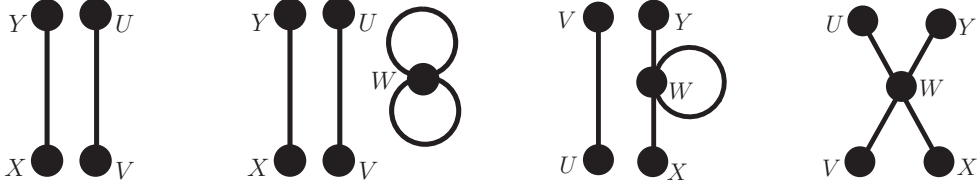


FIG. 2: Four-point function at leading order in $1/\kappa_4$.

The four-point function to first non-trivial order in $1/\kappa_4$ is given by

$$\langle \rho_x^a \rho_y^b \rho_u^c \rho_v^d \rangle \equiv \frac{\int \mathcal{D}\rho e^{-S_G[\rho]} \rho_x^a \rho_y^b \rho_u^c \rho_v^d \left[1 - \frac{1}{\kappa_4} \int d^2w \rho_w^a \rho_w^a \rho_w^b \rho_w^b \right]}{\int \mathcal{D}\rho e^{-S_G[\rho]} \left[1 - \frac{1}{\kappa_4} \int d^2w \rho_w^a \rho_w^a \rho_w^b \rho_w^b \right]}. \quad (24)$$

The different type of contractions which arise at this order are shown in Fig. 2. Eq. (24) then gives

$$\begin{aligned} \langle \rho_x^a \rho_y^b \rho_u^c \rho_v^d \rangle &= \frac{1}{1 - \frac{\mu^4}{\kappa_4} (N_c^2 + 1) (N_c^2 - 1) \frac{N_s}{\Delta^2 x}} \\ &\left\{ \frac{\mu^4}{(\Delta^2 x)^2} (\delta^{ab} \delta_{xy} \delta^{cd} \delta_{uv} + \delta^{ac} \delta_{xu} \delta^{bd} \delta_{yv} + \delta^{ad} \delta_{xv} \delta^{bc} \delta_{yu}) \left[1 - \frac{\mu^4}{\kappa_4} (N_c^2 + 1) (N_c^2 - 1) \frac{N_s}{\Delta^2 x} - 8 \frac{\mu^4}{\kappa_4} (N_c^2 + 1) \frac{1}{\Delta^2 x} \right] \right. \\ &\left. - 8 \frac{\mu^8}{\kappa_4 (\Delta^2 x)^3} (\delta^{ab} \delta^{cd} + \delta^{ac} \delta^{bd} + \delta^{ad} \delta^{bc}) \delta_{xy} \delta_{xu} \delta_{uv} \right\}. \quad (25) \end{aligned}$$

The second line in this expression corresponds to the sum of the first three diagrams shown in Fig. 2: the second term due to the disconnected diagram again cancels against the overall normalization factor once the latter is expanded to leading order in $1/\kappa_4$. Also, the third term from the second line is again absorbed into the renormalized value of μ^2 as in (20). In fact such a factor of $1 - 16 \frac{\mu^4}{\kappa_4} (N_c^2 + 1) \frac{1}{\Delta^2 x}$ appears at order $1/\kappa_4^2$ from diagrams of the type shown in Fig. 3 which induce the shift $\mu^8 \rightarrow \tilde{\mu}^8$ in the last line of eq. (25). Thus, the four-point function to order $1/\kappa_4$ finally becomes (switching again from lattice to continuum notation)

$$\begin{aligned} \langle \rho_x^a \rho_y^b \rho_u^c \rho_v^d \rangle &= \tilde{\mu}^4 \left[\delta^{ab} \delta^{cd} \delta(x-y) \delta(u-v) \left(1 - 8 \frac{\tilde{\mu}^4}{\kappa_4} \delta(x-u) \right) + \delta^{ac} \delta^{bd} \delta(x-u) \delta(y-v) \left(1 - 8 \frac{\tilde{\mu}^4}{\kappa_4} \delta(x-y) \right) \right. \\ &\left. + \delta^{ad} \delta^{bc} \delta(x-v) \delta(y-u) \left(1 - 8 \frac{\tilde{\mu}^4}{\kappa_4} \delta(x-y) \right) \right] \quad (26) \end{aligned}$$

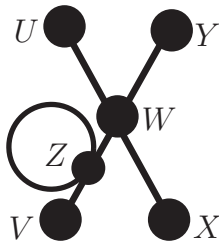


FIG. 3: Diagram at order $1/\kappa_4^2$ which renormalizes μ^2 in the connected contribution to the four-point function.

In momentum space,

$$\begin{aligned} \langle \rho^{*a}(k_1) \rho^{*b}(k_2) \rho^c(k_3) \rho^d(k_4) \rangle = & \\ (2\pi)^4 \tilde{\mu}^4 \left[\delta^{ab} \delta^{cd} \delta(k_1 + k_2) \delta(k_3 + k_4) + \delta^{ac} \delta^{bd} \delta(k_1 - k_3) \delta(k_2 - k_4) + \delta^{ad} \delta^{bc} \delta(k_1 - k_4) \delta(k_2 - k_3) \right. & \\ \left. - \frac{2}{\pi^2} \frac{\tilde{\mu}^4}{\kappa_4} (\delta^{ab} \delta^{cd} + \delta^{ac} \delta^{bd} + \delta^{ad} \delta^{bc}) \delta(k_1 + k_2 - k_3 - k_4) \right]. & \quad (27) \end{aligned}$$

V. CORRELATED TWO-GLUON PRODUCTION

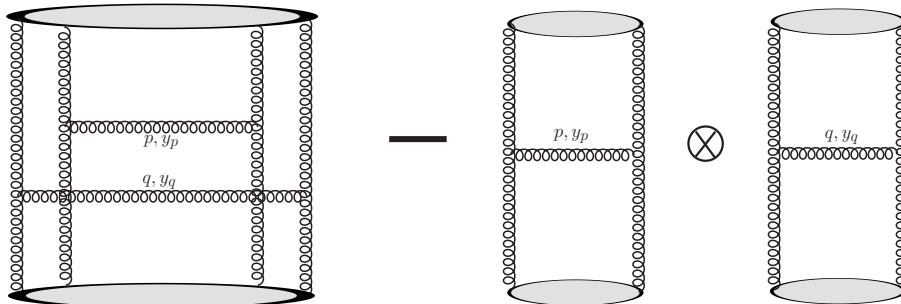


FIG. 4: Correlated production of two gluons with small relative azimuth, $\Delta\phi \ll \pi$.

We now turn to the color factor for correlated production of two gluons as illustrated in Fig. 4. We focus, in particular, on the so-called “ridge” kinematics where the gluons are separated by a rapidity interval $\Delta\eta \gtrsim 1$ but where their transverse momenta are nearly parallel so that their relative azimuth $\Delta\phi \ll \pi$. We assume that in this kinematic regime the dominant contribution arises from a process where the small- x gluons are produced from two separate ladders which connect to the same hard sources, though [10].

It was pointed out in ref. [12] that the cross section for this process involves a product of two four-point functions (projectile and target, respectively) such as the one discussed above. Further, that for a Gaussian action the correlated contribution which is left over after one subtracts the square of the single inclusive cross section is suppressed by $\sim 1/N_c^2$.

The diagram from Fig. 4 corresponds to [12]

$$f_{eaa'} f_{e'bb'} f_{ecc'} f_{e'dd'} \left\langle \rho^{*a}(k_2) \rho^{*b}(k_4) \rho^c(k_1) \rho^d(k_3) \right\rangle \left\langle \rho^{*a'}(p - k_2) \rho^{*b'}(q - k_4) \rho^{c'}(p - k_1) \rho^{d'}(q - k_3) \right\rangle \quad (28)$$

with e and e' , respectively, the color indices of the two produced gluons; the ladder momenta k_i will be integrated over. The (squared) single-inclusive cross section is obtained from

$$\begin{aligned} & f_{eaa'} f_{e'bb'} f_{ecc'} f_{e'dd'} \left\langle \rho^{*a}(k_2) \rho^c(k_1) \right\rangle \left\langle \rho^{*b}(k_4) \rho^d(k_3) \right\rangle \left\langle \rho^{*a'}(p - k_2) \rho^{c'}(p - k_1) \right\rangle \left\langle \rho^{*b'}(q - k_4) \rho^{d'}(q - k_3) \right\rangle \\ = & (2\pi)^4 N_c^2 (N_c^2 - 1)^2 (\pi R^2)^2 \tilde{\mu}^8 \delta(k_1 - k_2) \delta(k_3 - k_4). \quad (29) \end{aligned}$$

Translational invariance in the transverse plane brings along a factor of $\delta(k=0) = \pi R^2/(2\pi)^2$ for each of the two produced gluons. Using (15) the prefactor is of order

$$(\text{single inclusive})^2 \sim N_c^2(N_c^2 - 1)^2 (\pi R^2)^2 \left(\frac{g^2 A}{\pi R^2}\right)^4 \sim (gA^{1/3})^8 N_c^2(N_c^2 - 1)^2. \quad (30)$$

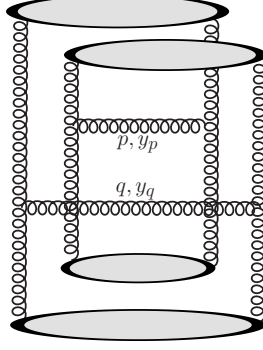


FIG. 5: Two-gluon production diagram which gives an angular collimation about $\Delta\phi = 0$ over several units in relative rapidity, $|y_p - y_q| \gtrsim 1$ (the so-called “ridge”) [8]. Such diagrams arise from a Gaussian action and only involve the two-point function (unintegrated gluon distribution); they are suppressed by $\sim 1/(N_c^2 - 1)$ relative to uncorrelated production.

The remaining contractions in eq. (28) generate connected diagrams corresponding to correlated production. In the limit $\kappa_4 \rightarrow \infty$ they are suppressed by a factor $1/(N_c^2 - 1)$. For example, for the diagram from fig. 5,

$$\begin{aligned} & f_{eaa'} f_{e'bb'} f_{ecc'} f_{e'dd'} \langle \rho^{*a}(k_2) \rho^d(k_3) \rangle \langle \rho^{*b}(k_4) \rho^c(k_1) \rangle \langle \rho^{*a'}(p - k_2) \rho^{c'}(p - k_1) \rangle \langle \rho^{*b'}(q - k_4) \rho^{d'}(q - k_3) \rangle \\ &= (2\pi)^6 N_c^2(N_c^2 - 1) \pi R^2 \tilde{\mu}^8 \delta(k_1 - k_2) \delta(k_3 - k_4) \delta(k_1 - k_4). \end{aligned} \quad (31)$$

Due to the additional δ -function as compared to eq. (29) there is, of course, only one single independent ladder momentum to integrate over. This diagram will therefore depend on the relative azimuthal angle between \mathbf{p} and \mathbf{q} ; it is proportional to

$$\text{Fig. 5} \sim N_c^2(N_c^2 - 1) \pi R^2 \frac{\tilde{\mu}^8}{p^2 q^2} \int \frac{dk^2}{k^4} \frac{1}{(p - k)^2} \frac{1}{(q - k)^2}. \quad (32)$$

Its contribution is therefore maximal at $\Delta\phi = 0$ and minimal at $\Delta\phi = \pi/2$ [8]. Also, the integral is quadratically divergent from the region $k^2 \ll p^2, q^2$ and $\mathbf{k} \sim \mathbf{p} \sim \mathbf{q}$. If a fixed non-perturbative cutoff Λ^2 is used then this contribution is $\sim A^2$, i.e., suppressed by $\sim A^{-2/3}$ as compared to uncorrelated production, eq. (30). On the other hand, if such cutoff is in fact provided by the non-linear saturation scale [10], $Q_s^2 \sim A^{1/3}$, then (31) is of order $\sim A^{5/3}$, down by A^{-1} as compared to uncorrelated production³.

For finite κ_4 , however, we can see from eq. (26,27) that the term $\sim \delta^{ac} \delta^{bd}$ produces the same overall color factor as the square of the single-inclusive cross section. The leading order (in $1/\kappa_4$) connected contribution of order $N_c^2(N_c^2 - 1)^2$ to (28) is shown diagrammatically in fig. 6 and is given by⁴

$$\begin{aligned} & -2(2\pi)^8 \frac{2}{\pi^2} \frac{\tilde{\mu}^8}{\kappa_4} \tilde{\mu}^4 \delta^{ac} \delta^{bd} \delta^{a'c'} \delta^{b'd'} f_{eaa'} f_{e'bb'} f_{ecc'} f_{e'dd'} \delta(k_1 - k_2) \delta(k_3 - k_4) \delta(k_1 + k_3 - k_2 - k_4) \\ &= -(2\pi)^6 \frac{4}{\pi^2} N_c^2(N_c^2 - 1)^2 \pi R^2 \frac{\tilde{\mu}^{12}}{\kappa_4} \delta(k_1 - k_2) \delta(k_3 - k_4). \end{aligned} \quad (33)$$

³ Note that in practice this $\sim 1/A$ suppression of the correlated contribution is usually removed by multiplying with the multiplicity per unit rapidity, dN/dy .

⁴ The overall factor of 2 accounts for projectile \leftrightarrow target flip.

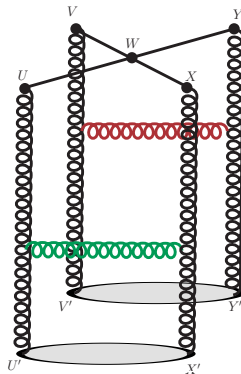


FIG. 6: Diagram for correlated two-gluon production from the quartic action. This contribution is of the same order in g^2 and A as that from fig. 5 but enhanced by a factor of $N_c^2 - 1$.

The contribution from this diagram to the two-particle spectrum is

$$\begin{aligned} &\sim -N_c^2(N_c^2 - 1)^2 \pi R^2 \frac{\tilde{\mu}^{12}}{\kappa_4} \frac{1}{p^2 q^2} \int \frac{dk^2}{k^2} \frac{1}{(p-k)^2} \int \frac{dk'^2}{k'^2} \frac{1}{(q-k')^2} \\ &\sim -N_c^2(N_c^2 - 1)^2 \pi R^2 \frac{\tilde{\mu}^{12}}{\kappa_4} \left(\frac{1}{p^2 q^2} \right)^2 \log \frac{p^2}{\Lambda^2} \log \frac{q^2}{\Lambda^2}. \end{aligned} \quad (34)$$

Thus, this contribution is independent of the azimuthal angle $\Delta\phi$ between \mathbf{p} and \mathbf{q} . Also, its sensitivity to the infrared cutoff is only logarithmic and would therefore not modify the A -dependence of the prefactor.

From (15) then the prefactor of (33) is of order

$$\text{Fig. 6} \sim N_c^2(N_c^2 - 1)^2 \pi R^2 \left(\frac{g^2 A}{\pi R^2} \right)^6 \frac{1}{g^4} \left(\frac{\pi R^2}{A} \right)^3 \sim g^8 A^{5/3} N_c^2(N_c^2 - 1)^2. \quad (35)$$

This is of the same order in g^2 and N_c as the uncorrelated contribution (30) but suppressed by one power of the mass number A . However, it is more relevant to compare the contribution from the quartic interaction to the correlation, eq. (35), to that from the Gaussian action, eq. (32). If the latter is cut off at a constant, A -independent scale Λ^2 then it is parametrically enhanced by a factor of $A^{1/3}$ and the corrections from the quartic term in the action can be computed perturbatively (near $A = \infty$) by an expansion in $1/\kappa_4$ (as we have done). One may expect that such corrections are large when $A^{1/3} \simeq 6$ since they are enhanced by a factor of $N_c^2 - 1$.

On the other hand, if the infrared cutoff $\sim Q_s^2 \sim A^{1/3}$ then the non-Gaussian action generates “corrections” to two-particle correlations which appear at the same order in A as the contribution from the Gaussian action (up to logarithms of A); in addition, those “corrections” are enhanced by a large color factor $N_c^2 - 1$. This case requires a non-perturbative calculation of the correlation to all orders in $1/\kappa_4$.

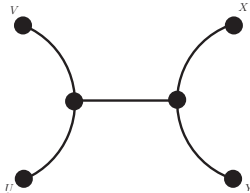


FIG. 7: Connected contribution to the four-point function at order $1/\kappa_3^2$.

We conclude this section by noting that the “odderon” operator can also contribute to the connected two-particle production cross section at order $\sim 1/\kappa_3^2$. This contribution is obtained by expanding the exponential of the odderon operator to second order. Performing the averaging of the four-point function shown in fig. 7 over the hard color

sources like in eq. (24) results in five Wick contractions and is of order μ^{10}/κ_3^2 . Multiplying by the leading $\sim \kappa_3^0$ contribution from the target side gives, in all:

$$+ \pi R^2 N_c^2 (N_c^2 - 1) \left(N_c - \frac{4}{N_c} \right) \frac{\tilde{\mu}^{14}}{\kappa_3^2} \sim + g^8 A^{5/3} N_c^2 (N_c^2 - 1) \left(N_c - \frac{4}{N_c} \right). \quad (36)$$

This is of the same order in A as the contribution $\sim 1/\kappa_4$ from eq. (35) although it is suppressed by one power of N_c . It appears sensible that numerical solutions of JIMWLK evolution also include the odderon operator in the action for the initial condition. On the other hand, terms of order $\sim \rho^6$ do not matter for the four-point function (they do matter for the six-point function and higher), they simply renormalize κ_4 .

VI. SUMMARY

In summary, we have computed corrections to the quadratic MV-model action up to quartic order in the density of hard (large- x) sources. Such terms are accompanied by additional powers of $1/gA^{1/3}$. This action could be employed to determine initial conditions for the JIMWLK high-energy evolution of various n -point operator expectation values. We have motivated this by showing that at leading order in the quartic coupling this action gives a connected contribution to two-gluon production (i.e., to correlations) already at leading order in N_c , enhanced by a factor of $N_c^2 - 1$ over the connected contribution from a (local) quadratic action. Such non-Gaussian actions may also be important for applications to dijet production with transverse momenta not very far above the saturation scale [19].

Acknowledgments

We thank S. Jeon for extensive discussions on the derivation of the MV action in ref. [5] and A. Kovner for communications which initiated this work. We gratefully acknowledge support by the DOE Office of Nuclear Physics through Grant No. DE-FG02-09ER41620, from the ‘‘Lab Directed Research and Development’’ grant LDRD 10-043 (Brookhaven National Laboratory), and from The City University of New York through the PSC-CUNY Research Award Program, grants 63382-0041 (A.D.) and 63404-0041 (J.J.M.).

VII. APPENDIX

In this appendix we illustrate how one can express the values of various Casimirs in terms of the Dynkin labels n and m of $SU(3)$. The representation (m, n) is reached by multiplying the $(1, 0)$ fundamental representation k times. The corresponding Young tableau thus has k boxes in $N = 3$ rows. The first row has $h_1 = m + n + (k - m - 2n)/3$ boxes; the second row has $h_2 = n + (k - m - 2n)/3$ boxes; and the last row has $h_3 = (k - m - 2n)/3$ boxes.

It is useful to define the set n'_i for the $U(N)$ group from these ‘‘row lengths’’ h_i via $n'_i = h_i + (N + 1)/2 - i$:

$$n'_1 = m + n + \frac{k - m - 2n}{3} + 2 - 1 = \frac{k + 2m + n}{3} + 1 \quad (37)$$

$$n'_2 = n + \frac{k - m - 2n}{3} + 2 - 2 = \frac{k - m + n}{3} \quad (38)$$

$$n'_3 = \frac{k - m - 2n}{3} + 2 - 3 = \frac{k - m - 2n}{3} - 1 \quad (39)$$

$$\sum_i n'_i = k. \quad (40)$$

To pass from $U(3)$ to $SU(3)$ one needs to shift $n_i = n'_i - \sum_j n'_j/N$ to get

$$n_1 = \frac{2m + n}{3} + 1 \quad (41)$$

$$n_2 = \frac{-m + n}{3} \quad (42)$$

$$n_3 = \frac{-m - 2n}{3} - 1. \quad (43)$$

Therefore,

$$\sum_i n_i^2 = \frac{2}{3} (m^2 + n^2 + mn) + 2(m + n + 1) \quad (44)$$

$$\sum_i n_i^4 = \frac{2}{9} (3 + m^2 + n^2 + 3n + 3m + mn)^2 . \quad (45)$$

The quadratic casimir is constructed from n_i via [20]⁵

$$C_2(m, n) = \sum_i n_i^2 - \frac{N(N^2 - 1)}{12} = \frac{1}{3} (m^2 + n^2 + mn) + (m + n) . \quad (46)$$

For a single quark corresponding to the fundamental representation ($m = 1, n = 0$) of QCD, we get $C_2 = (N_c^2 - 1)/(2N_c) = 4/3$.

To compute the cubic Casimir we require the set of $l_i = n_i + (N - 1)/2$,

$$l_1 = \frac{2m + n}{3} + 2 \quad (47)$$

$$l_2 = \frac{-m + n}{3} + 1 \quad (48)$$

$$l_3 = \frac{-m - 2n}{3} \quad (49)$$

$$\sum_i l_i = N \quad (50)$$

$$\sum_i l_i^2 = N + \sum_i n_i^2 = \frac{2}{3} (m^2 + n^2 + mn) + 2(m + n) + 5 \quad (51)$$

$$\sum_{i < j} l_i l_j = l_1(l_2 + l_3) + l_2 l_3 = 2 - \frac{2m + n}{3} - \frac{4m^2 + n^2 + 4mn}{9} - \frac{3m + 6n - nm + 2n^2 - m^2}{9} \quad (52)$$

$$= 2 - \frac{m^2 + n^2 + mn + 3m + 3n}{3} \quad (53)$$

$$\sum_i l_i^3 = \frac{2m^3 - 2n^3 + 3m^2 n - 3mn^2}{9} + 3m^2 + n^2 + 2mn + 7m + 5n + 9 . \quad (54)$$

These can then be used to construct the cubic Casimir following [20] and lead to

$$C_3(m, n) \equiv \frac{1}{18} (m + 2n + 3) (n + 2m + 3) (m - n) . \quad (55)$$

Constructing $C_4(m, n)$ requires the vectors n_i^4 and can be done similarly to $C_2(m, n)$; this leads to

$$C_4(m, n) \equiv \frac{1}{9} (m^4 + n^4 + 2mn^3 + 2m^3 n + 3m^2 n^2) + \frac{2}{3} (m^3 + n^3 + 2m^2 n + 2mn^2) + \frac{1}{6} (5m^2 + 5n^2 + 11mn) - \frac{1}{2} (m + n) . \quad (56)$$

[1] J. Jalilian-Marian, A. Kovner, L. D. McLerran and H. Weigert, Phys. Rev. D **55**, 5414 (1997); J. Jalilian-Marian, A. Kovner, A. Leonidov and H. Weigert, Nucl. Phys. B **504**, 415 (1997), Phys. Rev. D **59**, 014014 (1999), Phys. Rev. D **59**, 014015 (1999), Phys. Rev. D **59**, 034007 (1999) [Erratum-ibid. D **59**, 099903 (1999)]; A. Kovner, J. G. Milhano and H. Weigert, Phys. Rev. D **62**, 114005 (2000); A. Kovner and J. G. Milhano, Phys. Rev. D **61**, 014012 (2000); E. Iancu, A. Leonidov and L. D. McLerran, Nucl. Phys. A **692**, 583 (2001), Phys. Lett. B **510**, 133 (2001); E. Ferreiro, E. Iancu, A. Leonidov and L. McLerran, Nucl. Phys. A **703**, 489 (2002).

⁵ Note that their normalization of the generators is different from ours so that their expressions for the Casimirs need to be divided by 2.

- [2] I. Balitsky, Nucl. Phys. **B463**, 99-160 (1996) [hep-ph/9509348]; Y. V. Kovchegov, Phys. Rev. D **60**, 034008 (1999); Phys. Rev. D **61**, 074018 (2000).
- [3] L. D. McLerran, R. Venugopalan, Phys. Rev. **D49**, 2233-2241 (1994) [hep-ph/9309289]; Phys. Rev. **D49**, 3352-3355 (1994) [hep-ph/9311205].
- [4] P. Tribedy and R. Venugopalan, Nucl. Phys. **A850**, 136-156 (2011) [arXiv:1011.1895 [hep-ph]].
- [5] S. Jeon and R. Venugopalan, Phys. Rev. D **70**, 105012 (2004); Phys. Rev. D **71**, 125003 (2005).
- [6] V. Khachatryan *et al.* [CMS Collaboration], JHEP **1009**, 091 (2010) [arXiv:1009.4122 [hep-ex]].
- [7] J. Adams *et al.* [STAR Collaboration], Phys. Rev. Lett. **95**, 152301 (2005); J. Putschke, J. Phys. G **34**, S679 (2007); A. Adare *et al.* [PHENIX Collaboration], Phys. Rev. C **78**, 014901 (2008); B. I. Abelev *et al.* [STAR Collaboration], Phys. Rev. **C80**, 064912 (2009); B. Alver *et al.* [PHOBOS Collaboration], Phys. Rev. Lett. **104**, 062301 (2010).
- [8] A. Dumitru, K. Dusling, F. Gelis, J. Jalilian-Marian, T. Lappi, R. Venugopalan, Phys. Lett. **B697**, 21-25 (2011) [arXiv:1009.5295 [hep-ph]].
- [9] Y. V. Kovchegov, E. Levin, L. D. McLerran, Phys. Rev. **C63**, 024903 (2001) [hep-ph/9912367].
- [10] A. Dumitru, F. Gelis, L. McLerran and R. Venugopalan, Nucl. Phys. A **810**, 91 (2008) [arXiv:0804.3858 [hep-ph]].
- [11] K. Dusling, F. Gelis, T. Lappi and R. Venugopalan, Nucl. Phys. A **836**, 159 (2010) [arXiv:0911.2720 [hep-ph]].
- [12] A. Dumitru and J. Jalilian-Marian, Phys. Rev. D **81**, 094015 (2010) [arXiv:1001.4820 [hep-ph]].
- [13] A. Kovner, M. Lublinsky, Phys. Rev. **D83**, 034017 (2011) [arXiv:1012.3398 [hep-ph]].
- [14] A. H. Mueller, Nucl. Phys. **B643**, 501-513 (2002) [hep-ph/0206216]; Y. Hatta, A. H. Mueller, Nucl. Phys. **A789**, 285-297 (2007) [hep-ph/0702023 [HEP-PH]].
- [15] E. Levin, A. H. Rezaeian, [arXiv:1105.3275 [hep-ph]].
- [16] J. Bartels, M. G. Ryskin, [arXiv:1105.1638 [hep-ph]].
- [17] A. Dumitru, J. Jalilian-Marian, Phys. Rev. Lett. **89**, 022301 (2002) [hep-ph/0204028].
- [18] K. Rummukainen, H. Weigert, Nucl. Phys. **A739**, 183-226 (2004) [hep-ph/0309306]; Y. V. Kovchegov, J. Kuokkanen, K. Rummukainen, H. Weigert, Nucl. Phys. **A823**, 47-82 (2009) [arXiv:0812.3238 [hep-ph]]; T. Lappi, B. Schenke, R. Venugopalan, work in progress, private communication.
- [19] A. Dumitru, J. Jalilian-Marian, Phys. Rev. **D82**, 074023 (2010) [arXiv:1008.0480 [hep-ph]].
- [20] F. Dubath, S. Lelli and A. Rissone, Int. J. Mod. Phys. A **19**, 205 (2004) [arXiv:hep-th/0211133].